

Efficient modeling of shallow water equations using method of lines and artificial viscosity

Mohamed M. Mousa*

*Department of Mathematics,
College of Science and Human Studies at Hotat Sudair,
Majmaah University, Majmaah 11952, Saudi Arabia
Department of Basic Science, Faculty of Engineering at Benha,
Benha University, Benha 13512, Egypt
mm.mousa@mu.edu.sa*

Wen-Xiu Ma

*Department of Mathematics, Zhejiang Normal University,
Jinhua 321004, Zhejiang, China
Department of Mathematics, King Abdulaziz University,
Jeddah 21589, Saudi Arabia
Department of Mathematics and Statistics, University of South Florida,
Tampa, FL 33620, USA
College of Mathematics and Physics, Shanghai University of Electric Power,
Shanghai 200090, China
College of Mathematics and Systems Science,
Shandong University of Science and Technology, Qingdao 266590, China
Department of Mathematical Sciences, North-West University,
Ma Keng Campus, Mmabatho 2735, South Africa
maux@cas.usf.edu*

Received 10 August 2019

Revised 12 September 2019

Accepted 26 September 2019

Published 19 December 2019

In this work, two numerical schemes were developed to overcome the problem of shock waves that appear in the solutions of one/two-layer shallow water models. The proposed numerical schemes were based on the method of lines and artificial viscosity concept. The robustness and efficiency of the proposed schemes are validated on many applications such as dam-break problem and the problem of interface propagation of two-layer shallow water model. The von Neumann stability of proposed schemes is studied and hence, the sufficient condition for stability is deduced. The results were presented graphically. The verification of the obtained results is achieved by comparing them with exact solutions or another numerical solutions founded in literature. The results are satisfactory and in much have a close agreement with existing results.

Keywords: Shallow water equations; shock waves; method of lines; artificial viscosity.

*Corresponding author.

1. Introduction

Simulation of hyperbolic conservation equations is significant and remains a matter of intense research, especially, by the scientists of Computational Fluid Dynamics (CFD). It is well known that hyperbolic conservation equations model the physics of shallow water flows or gas dynamics. The motive is to develop a robust, yet accurate and stable numerical technique. Since the shallow water equations give rise to shock waves, contact discontinuities and also produce expansion waves with probable sonic points, any technique developed for such equations must be able to capture these features with appropriate accuracy without mislaying robustness. Also, the used numerical method should compute such discontinuities with the accurate position and without spurious oscillations and realize high-order of accuracy in the smooth areas too. In general, the techniques that used for the simulation of such systems are called shock-capturing methods.

From the literature, the methods of shock-capturing are categorized into two general groups: classical techniques and modern shock-capturing ones. Modern shock-capturing methods are commonly upwind based in contrast to central discretization. The upwind-type differencing schemes try to discretize the differential equations by differencing biased in the direction determined by the characteristic speeds sign. While, central or symmetric schemes don't consider any data about the propagation of the wave in the discretization. On other hand, the central discretization schemes are easier than the upwind ones, they regularly contain tuning parameters which are problem dependent. Also the main obstacle in using such classical central numerical schemes is the risk of generation of unphysical numerical fluctuations. Because of these disadvantages, upwind schemes and modern shock-capturing methods became more popular from 1970s. These modern shock-capturing schemes have a non-linear numerical dissipation, with an automatic feedback mechanism that adjusts the amount of dissipation in any cell of the mesh, in accord to the gradients in the solution. These schemes have proven to be accurate and stable even when the problem contains strong shock waves. Some of the famous classical techniques include the Godunov method,⁸ Lax–Wendroff method,¹⁸ the MacCormack method^{20,21} and the method of lines (MOL).^{9,22,23,27,28} Examples of modern shock-capturing schemes include higher-order total variation diminishing (TVD) method which firstly introduced by Harten,¹⁰ monotonic upstream-centered schemes for conservation laws (MUSCL) based on Godunov approach that introduced by Van Leer,³⁰ flux-corrected transport method presented by Boris and Book,² piecewise parabolic method (PPM) offered by Woodward and Colella⁴ and various essentially non-oscillatory schemes (ENO) suggested by Harten *et al.*¹¹ Of all the modern shock-capturing schemes, the approximate Riemann solver of Roe²⁶ is the most popular, as it can capture steady discontinuities exactly, without any numerical dissipation. Recently, many authors applied various numerical methods to solve and simulate many shallow water model.^{32–35}

Shallow water equations are generally used for modeling environmental fluid dynamics when the field of the flow has one component that is insignificant with respect to other components, e.g. the vertical velocity is small with respect to the longitudinal or lateral components. This is the so-called shallow water hypothesis, and is considered true once the process has a dominant characteristic dimension. Applications of shallow water equations vary from atmospheric circulation¹³ to tsunami wave propagation in oceans²⁴ and large-scale ocean modeling,¹² from river morph dynamics¹⁷ to granular flows and dam break.^{7,14–16} Recently, the justification of the applicability of shallow-water theory in the simulation of wave flows of fluid is discussed in Ref. 31. Multi-layer shallow water models are mainly useful in some limit cases of multi-fluids and variable density flows parted by nearly horizontal interfaces. These models govern the dynamics of incompressible fluids spreading under gravity effects. The most popular case of the multi-layer shallow water models is the system of two-layer shallow water equations. Such system is obtained by vertical averaging through each layer depth of compressible isentropic Euler equations. The water layers are supposed to have unequal constant densities $\rho_1 < \rho_2$, for example, difference in salinity of water, or to be immiscible. The considered two-layer shallow water equations are extensions of the Saint-Venant systems,⁵ which are commonly used in both dams-keeping engineering and geophysical science. Considering the one-dimensional two-layer shallow water model, see Fig. 1, that describes a flow, in a straightforward channel with a bottom topography $B(x)$, which consists of double layers of heights h_1 (upper layer) and h_2 (lower layer) at spatial x in any time t with corresponding velocities u_i and discharges $q_i = h_i u_i, i = 1, 2$. This

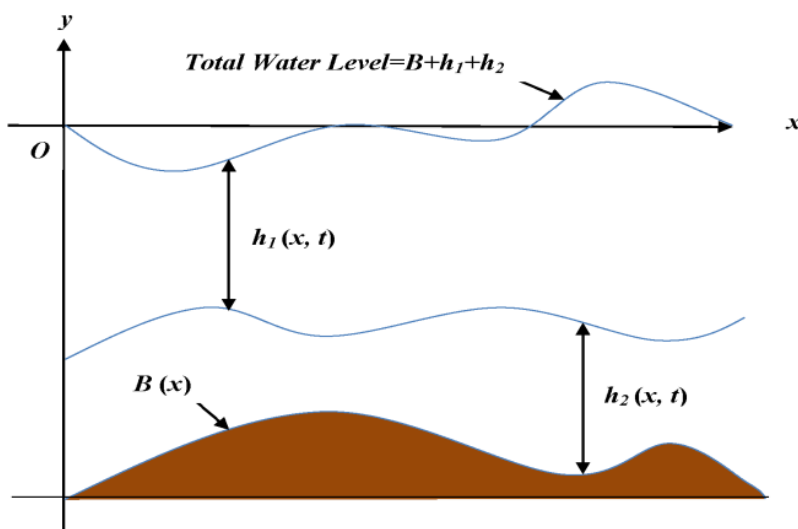


Fig. 1. (Color online) Two-layer shallow water structure.

model is studied in Refs. 3 and 16 and given by

$$\begin{aligned}
 (h_1)_t + (q_1)_x &= 0, \\
 (q_1)_t + \left(h_1 u_1^2 + \frac{g}{2} h_1^2 \right)_x &= -gh_1 B_x - gh_1 (h_2)_x, \\
 (h_2)_t + (q_2)_x &= 0, \\
 (q_2)_t + \left(h_2 u_2^2 + \frac{g}{2} h_2^2 \right)_x &= -gh_2 B_x - gr h_2 (h_1)_x,
 \end{aligned} \tag{1}$$

where γ is the constant of gravity and $r = \rho_1/\rho_2$ is the density ratio parameter. Accordingly, the one-dimensional form of single-layer shallow water equations can be written as

$$\begin{aligned}
 (h)_t + (hu)_x &= 0, \\
 (hu)_t + \left(hu^2 + \frac{g}{2} h^2 \right)_x &= -gh B_x(x).
 \end{aligned} \tag{2}$$

Here, h and u represent the water depth and the water velocity in x -direction respectively. Stimulating the solutions of system (1) and (2) is a difficult problem due to many causes: they include non-conservative product terms, their eigenstructure can't be obtained in an explicit form also the these systems are conditionally hyperbolic. Even though the previous factors make it quite difficult to develop a numerical scheme for such systems, the MOL with the aid of the artificial viscosity principle can be considered as an interesting approach to deal with these difficulties.

The solutions of the presented systems are obtained by the method of lines. It is known that the MOL is a classical shock-capturing approach which summarized as an approximations to the space derivatives in a partial differential equation (PDE) system and reducing the problem to an initial value ordinary differential equation (ODE) system and then using a robust time integrator to sol the resulting ODE system. The accuracy of the method can be enhanced using a highly reliable and robust ODE solvers. Although the MOL is considered as a classical approach, it will be stable and suitable even for strong shock waves problems. The numerical oscillations that may be raised across discontinuities will be avoided if an artificial viscosity term is added as we will see in the next sections.

This paper is partitioned into four sections. In Sec. 2, two numerical schemes with different order of accuracy, based on the method of lines and the artificial viscosity principle, are developed for system (2) to shortcut in writing. And hence, with the same principle, the numerical schemes for system (1) can be easily deduced. In Sec. 3 we consider the stability of the considered schemes for one-layer shallow water equation in the von Neumann sense. Section 4 contains the results of extensive numerical experiments on a set of five test numerical problems. Comparisons of the obtained results with analytical solutions and other numerical results in literature are presented as well. The considered test problems include the one-layer dam-break problem with and without a source term. Test problems of the two-layer shallow water equations with a variable depth riverbed are considered in Sec. 3 as well. In Sec. 4, the comments and conclusions are introduced.

2. Numerical Schemes Using Method of Lines and Artificial Viscosity

A detailed explanation of the MOL and their applications for solving various problems can be found in literature, e.g.^{9,22–24,27,28} No matter what type of numerical scheme will be used, a stable calculations, in existence of shock waves, need a certain amount of numerical dissipation to avoid the formation of the unphysical numerical oscillations that will be risen across discontinuities. The main idea of the artificial viscosity principle is adding a diffusion term (derivatives of second-order) to the central scheme that prevents the amplification of a solution in the proximity of surges (sharp gradients), i.e. it prevents the appearance of disturbances with small wavelength. In order to utilize the method of lines with the artificial viscosity principle for solving system (2), we set the discharge q as $q = hu$ and hence the second-order MOL scheme (MOL I) can be obtained by replacing the first and second derivatives with respect to x at every grid points $x_i, i = 1, 3, \dots, N - 1$, with the second-order central difference approximation as follows:

$$\begin{aligned} \frac{dh_i}{dt} &= -\frac{q_{i+1} - q_{i-1}}{2\Delta x} + \varepsilon \frac{h_{i-1} - 2h_i + h_{i+1}}{(\Delta x)^2}, \quad i = 1, 2, \dots, N - 1, \quad t \geq 0, \\ \frac{dq_i}{dt} &= -\frac{2h_i q_i \frac{q_{i+1} - q_{i-1}}{2\Delta x} - q_i^2 \frac{h_{i+1} - h_{i-1}}{2\Delta x}}{(\Delta x)^2} \\ &\quad - g h_i \left(\frac{h_{i+1} - h_{i-1}}{2\Delta x} + B_x(i\Delta x) \right) + \varepsilon \frac{q_{i-1} - 2q_i + q_{i+1}}{(\Delta x)^2}. \end{aligned} \quad (3)$$

where i represents the cell centroid, N is the number of the grid points, Δx is the space step and ε is a parameter associated to the artificial viscosity term. Eq. (3) is a second-order central finite difference approximation of Eq. (2) after replacing the flux hu with the discharge q and adding the artificial viscosity terms εh_{xx} and εq_{xx} . It is noted that^{23,24} the choice of ε is somewhat arbitrary, and must be selected upon the solution shock waves strength. Preferably, ε need to be sufficiently small i.e. $\varepsilon \ll 1$. Throughout the remainder of this paper, ε is set to 10^{-3} and γ is set to 9.81 except in problem 3. The classical fourth-order Runge–Kutta (RK4) method has been used as a time integrator to solve the system of ODEs (3) corresponding to the given initial/boundary conditions using a suitable time step Δt .

In order develop the fourth-order MOL scheme (MOL II), we replaced the first and second derivatives approximations in system (3) with the fourth-order central difference approximations as follows:

$$\begin{aligned} \frac{f_{i+1} - f_{i-1}}{2\Delta x} &\rightarrow \frac{f_{i-2} - 8f_{i-1} + 8f_{i+1} - f_{i+2}}{12\Delta x}, \\ \frac{f_{i-1} - 2f_i + f_{i+1}}{(\Delta x)^2} &\rightarrow \frac{-f_{i-2} + 16f_{i-1} - 30f_i + 16f_{i+1} - f_{i+2}}{12(\Delta x)^2} \end{aligned} \quad (4)$$

where f_i represent the dependent variables h_i and q_i in system (3).

3. Von Neumann Stability Analysis of MOL I Scheme

In this section, we study the von Neumann stability condition when using a central second-order discretization for spatial approximation together with forward time discretization. In order to investigate the von Neumann stability, we will linearize the homogeneous type of the single-layer shallow water equation (2) about a constant state $(h, q) = (\bar{h}, \bar{h}\bar{u})$ as done in Ref. 25:

$$\partial_t v + A \partial_x v = \varepsilon \partial_{xx} v, \quad A = \begin{pmatrix} 0 & 1 \\ \bar{c}^2 - \bar{u}^2 & 2\bar{u} \end{pmatrix}, \quad (5)$$

with $v = (h, q)^T$, $\bar{c} = \sqrt{P'(\bar{h})}$ and $P(\bar{h}) = \frac{g}{2}\bar{h}^2$. By denoting the approximations v_j^n to the values $v(x_j, t_n)$ at mesh points $x_j = j\Delta x, j \in \mathbb{N}$ and $t_n = n\Delta t, n \in \mathbb{N}$, where Δt denotes the time step. Using a central difference in space and the forward discretization in time, system (5) will have the following formulation:

$$v_j^{n+1} = v_j^n - \frac{a}{2}(v_{j+1}^n - v_{j-1}^n) + b(v_{j+1}^n - 2v_j^n + v_{j-1}^n), \quad (6)$$

where $a = \frac{\|A\|\Delta t}{\Delta x}$ and $b = \frac{\varepsilon\Delta t}{\Delta x^2}$.

Based on the von Neumann analysis, the numerical solutions v_j^{n+1} are decomposed into a Fourier series as,

$$v_j^n = \sum_{q=-N}^N k_q^n e^{i\xi_q(j\Delta x)}, \quad (7)$$

where $i = \sqrt{-1}$ and k_q^n is the amplification factor at q th harmonic and $\xi_q = q\pi/N\Delta x$. The product $\xi_q\Delta x$ is the phase angle $\theta = \xi_q\Delta x$ where $\theta \in [-\pi, \pi]$ in steps of π/N . The time evolution of a single mode $k^n e^{ij\theta}$ can be determined by the same numerical scheme as the complete numerical solution v_j^n . Therefore, by inserting a representation of this formula into a numerical scheme we can obtain a stability condition by imposing an upper bound to the amplification factor k .

It is known that two level linear finite difference method is stable in the l_2 -norm if and only if the von Neumann condition is satisfied. And the amplification factor is said to satisfy the von Neumann condition if the following practical or strict stability condition is satisfied:

$$|k(\theta)| \leq 1 \quad \forall \theta \in [-\pi, \pi]. \quad (8)$$

Substituting $v_j^n = \sum k^n(\theta) e^{ij\theta}$, into the scheme (6) yields,

$$k(\theta) = 1 - ia \sin(\theta) + 2b(\cos(\theta) - 1), \quad -\pi \leq \theta \leq \pi. \quad (9)$$

If we consider the function $M(\theta) = |k(\theta)|^2$, then we have

$$M(\theta) = [1 + 2b(\cos(\theta) - 1)]^2 + a^2[1 - \cos^2(\theta)]. \quad (10)$$

The maximum of the function M in terms of $\cos \theta$ can be obtained by differentiating $M(\theta)$ with respect to $\cos \theta$ and it can simply founded that a maximum occurs only

if $8b^2 - 2a^2 < 0$, that is, if $a > 2b$. Also, the maximum or minimum occurs for

$$\cos(\theta) = \frac{2b(1-2b)}{a^2 - 4b^2}. \quad (11)$$

Substituting Eq. (11) into Eq. (10), yields

$$M(\theta) = \frac{a^2(a^2 + 1 - 4b)}{a^2 - 4b^2}. \quad (12)$$

So, the condition in Eq. (8) together Eq. (12) implies $a^2 - 4b^2 \leq 0$. When $a > 2b$, this condition can't be met; and therefore we must first consider

$$a \leq 2b. \quad (13)$$

If Eq. (13) satisfied, no maximum of the function M is occurred, and hence we have to consider the end values of $\cos(\theta)$. So if $\cos(\theta) = 1$, then the function $M(\theta) = 1$ and stability is achieved. But when $\cos(\theta) = -1$, the following condition can simply obtained

$$2b \leq 1. \quad (14)$$

Therefore the stability condition can be obtained from Eq. (13) and Eq. (14) as,

$$a \leq 2b \leq 1. \quad (15)$$

4. Test Problems

In order to validate the dependability and efficiency of the considered schemes, we test them on four numerical examples in one and two dimensions. The examples are considered as bench-mark test problems for numerical methods. We have validated the presented numerical results by comparing them with exact solutions or other numerical ones exists in literature.

4.1. Problem 1

The first test problem is 1-D dam-break problem that was discussed in Ref. 14 and Ref. 29. Consider the initial-value problem of Eq. (2) with no source term. This occurred because of the river-bed being of fixed depth and hence resulting in $B_x(x) = 0, \forall x$. We also have the following initial conditions:

$$u(x, 0) = 0 \quad \text{and} \quad h(x, 0) = \begin{cases} 1, & \text{for } 0 \leq x \leq 0.5, \\ 0.5, & \text{for } 0.5 < x \leq 1. \end{cases} \quad (16)$$

Here, the existence of discontinuity at $x = 0.5$ is similar to a barrier separating two river heights. For this test problem, step-sizes $\Delta x = 0.002$ and $\Delta t = 0.001$ will be used with a final time of $t = 0.1$. A comparison between the obtained result and the exact solution¹⁴ of the water depth will be displayed at $t = 0.02 i$, where $i = 0$ to 5. Results, of MOL I and MOL II schemes, presented in Fig. 2 show all the flow features being captured well and closer agreement with the exact solution is noticed.

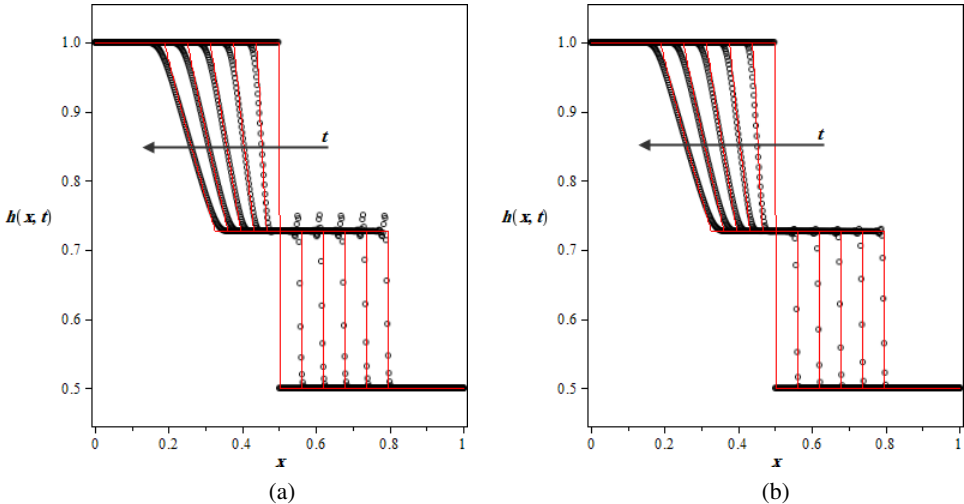


Fig. 2. (Color online) Plot of the water depth $h(x, t)$ at $t = 0.02 i$, where $i = 0$ to 5 using (a) MOL I results and (b) MOL II results and exact solution (solid lines) for problem 1.

As it can be seen from Fig. 2, the results of the both schemes are well agreed with the exact solution. Also, we can see small non-physical oscillations behind the shock fronts in case of using the MOL I scheme and hence the results obtained by MOL I, has a little accuracy when compared by those obtained by MOL II at the same parameters. It is worth noticing that since the discretization in the method of lines is applied only to the spatial variable, increasing the final time doesn't reduce the solution accuracy and better results can be obtained by using a more sensitive integrator for solving the system of ODEs, however in classical finite difference techniques, there are usually limitations when final time growths.

4.2. Problem 2

The second problem is a 1-D dam-break problem on a variable depth river-bed that was discussed in Refs. 14 and 15. In this test example we considered the initial-value problem of Eq. (2) with variable river-bed and so the system of equations is nonhomogeneous, which means that a source term is present in the system. As considered in Refs. 14 and 15, the bottom topography of the river-bed is defined as,

$$B(x) = \begin{cases} 0.125[\cos(10\pi(x - 0.5)) + 1], & \text{for } 0.4 \leq x \leq 0.6, \\ 0, & \text{otherwise,} \end{cases} \quad (17)$$

and considering the following initial conditions:

$$u(x, 0) = 0 \quad \text{and} \quad h(x, 0) = \begin{cases} 1 - B(x), & \text{for } 0 \leq x \leq 0.5, \\ 0.5 - B(x), & \text{for } 0.5 < x \leq 1. \end{cases} \quad (18)$$

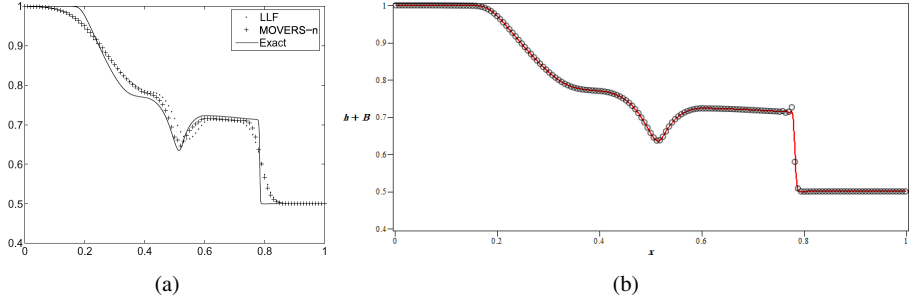


Fig. 3. (Color online) Comparison between (a) results obtained in Ref. 15 and (b) numerical results of MOL I (circles) and MOL II (line) for the water depth ($h + B$) at $t = 0.1$ for problem 2.

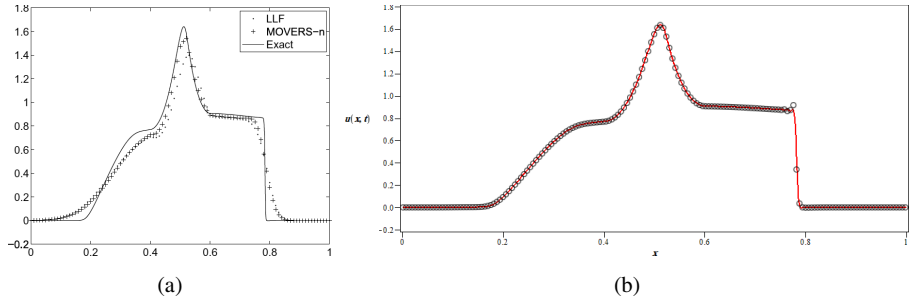


Fig. 4. (Color online) Comparison between (a) results obtained in Ref. 15 and (b) numerical results of MOL I (circles) and MOL II (line) for the water velocity at $t = 0.1$ for problem 2.

Here, step-sizes will be taken as in problem 1 and the final time is considered to be $t = 0.1$. A comparison between the obtained results and the numerical results obtained in Ref. 15 for both water depth and velocity will be displayed for $t = 0.1$ in Figs. 3 and 4. Moreover, for more validation, in Fig. 5, the water velocity profile using the MOL II results are compared with the results mentioned in Ref. 14.

From Figs. 2–5, it can be concluded that the MOL I and MOL II schemes can capture the flow features of the dam-break flow even with bottom topography in a good manner and their results are very satisfactory due to the excellent agreement with the exact/previous results.

4.3. Problem 3

In this problem, we study the interface propagation of 1-D two-layer shallow water model that can be described from Eq. (1) and Fig. 1. The considered problem is taken from¹⁶ which is a slight variation of the test problem 2 from.³ The aim here is to capture the shock wave propagation of the two-layer interface, initially located at $x = 0.3$ by considering the following initial conditions:

$$(h_1, q_1, h_2, q_2)(x, 0) = \begin{cases} (0.50, 1.25, 0.50, 1.25), & \text{for } x \leq 0.3, \\ (0.45, 1.125, 0.55, 1.375), & \text{for } x > 0.3. \end{cases} \quad (19)$$

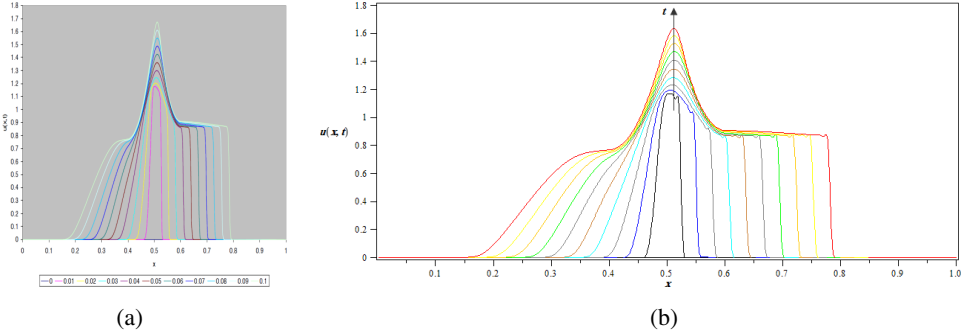


Fig. 5. (Color online) Comparison between (a) results obtained in Ref. 14 and (b) numerical results of MOL II for the water velocity at $t = 0.01 i$, where $i = 0$ to 10 for problem 2.

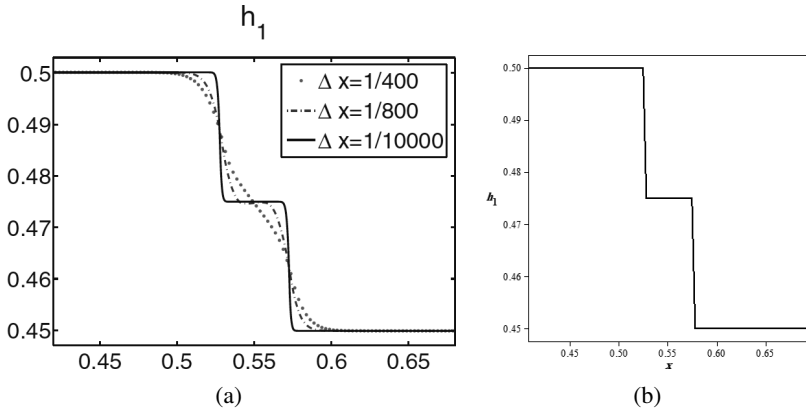


Fig. 6. Comparison between (a) results obtained in Ref. 16 and (b) numerical results of MOL II for the upper layer height (h_1) at $t = 0.1$ for problem 3.

In this problem, the bottom topography is considered to be flat ($B = -1$), the density ratio parameter is $r = 0.98$ and the gravitational constant is $\gamma = 10$. The step-sizes are taken very small, for high resolution calculations, as $\Delta x = 10^{-4}$, $\Delta t = 5 \times 10^{-5}$ and artificial viscosity is considered as $\varepsilon = 10^{-4}$. Here, the numerical solution is computed using the MOL II scheme at time $t = 0.1$. The numerical results obtained in Ref. 16 serve as a reference solution for this problem since the exact solution is unavailable.

The obtained results, using the MOL II scheme, for upper layer height h_1 , total water level ζ and upper layer velocity u_1 are shown in Figs. 6–8. As one may clearly see in Fig. 6, that a transitional flat state ($h_1 \approx 0.475$) has occurred. It is coupled to the left state ($h_1 = 0.5$) and right state ($h_1 = 0.45$) through two waves that look to be shock discontinuities. From Figs. 6–8, it can be clearly seen that the initial sharp interface produces four waves traveling with four various characteristic speeds. Moreover, it can be shown that there are no numerical oscillations appear when

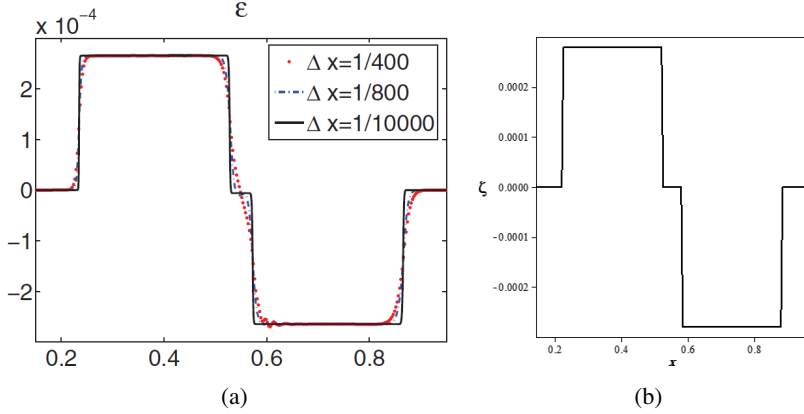


Fig. 7. (Color online) Comparison between (a) results obtained in Ref. 16 and (b) numerical results of MOL II for the total water level ($\zeta = h_1 + h_2 + B$) at $t = 0.1$ for problem 3.

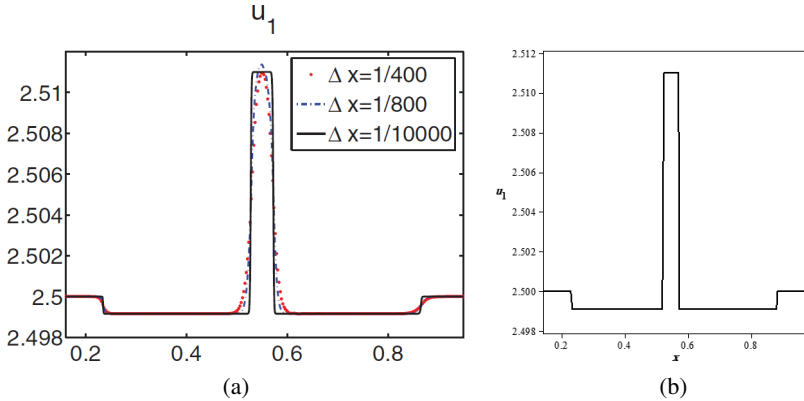


Fig. 8. (Color online) Comparison between (a) results obtained in Ref. 16 and (b) numerical results of MOL II for the upper layer velocity (u_1) at $t = 0.1$ for Problem 3.

using high resolution parameters and an excellent agreement, between obtained results and results were reported in Ref. 16, are noticed.

4.4. Problem 4

In this problem, we study a widely used problem for 2-D partial dam-break simulations. In this test case the computational domain is considered as a scaled one from the widely case considered in Refs. 1, 6, 15 and 19. Here, the computational domain is 1 m wide and 1 m. A dam with a thickness of 0.02 m divides the domain into two equal parts at $x = 0.5$ m. Initially, the upstream water depth was 1 m, while the downstream water depth was set to 0.5 m. We considered two cases of the dam breach, (i) the breach in the dam started from $y = 0.47$ m and ended at $y = 0.84$ m and (ii) the breach in the dam is occurred in middle and started from $y = 0.31$ m

and ended at $y = 0.68$ m. The bed is considered to be flat and frictionless. The water surface was analyzed graphically at 0.13 s after the breach in the dam was occurred. The 2-D shallow water equations with flat bed can be written as:

$$\begin{aligned} (h)_t + (hu)_x + (hv)_y &= 0, \\ (hu)_t + \left(hu^2 + \frac{g}{2} h^2 \right)_x + (huv)_y &= 0, \\ (hv)_t + \left(hv^2 + \frac{g}{2} h^2 \right)_y + (huv)_x &= 0, \end{aligned} \quad (20)$$

where v is the velocity component in y -direction. In this problem, the bottom topography is considered to be flat and the gravitational constant is $\gamma = 9.81$. A grid of 60×60 cells is used for this problem and time step-size is taken as $\Delta t = 5 \times 10^{-5}$ while the artificial viscosity is considered as $\varepsilon = 10^{-3}$. Here, the solution is calculated using the MOL I scheme at time $t = 0.13$. There is no analytical reference solution for this test problem, but in the literature numerical results of many authors are available (e.g.^{1,6,15,19}). The behavior of the MOL I schemes is in good agreement with computed results of these authors. The numerical results displaying 3-D views of the water depth after dam failure and depth contours at time $t = 0.13$ s are presented in Fig. 9 for case (i) and Fig. 10 for case (ii). At the moment the dam-breaks, water is released over the breach, establishing a positive wave that propagates downstream and a negative wave that moves upstream. The results shown in Figs. 9 and 10 are in satisfactory agreement with the results obtained by other numerical techniques in above-mentioned literatures.

At the end, one can notice that the novelty and the significance of the results are summarized in the following: (i) deducing von Neumann sufficient condition for stability of the proposed MOL schemes when using an artificial viscosity term and (ii) demonstrating the efficiency, robustness, and accuracy of the MOL with

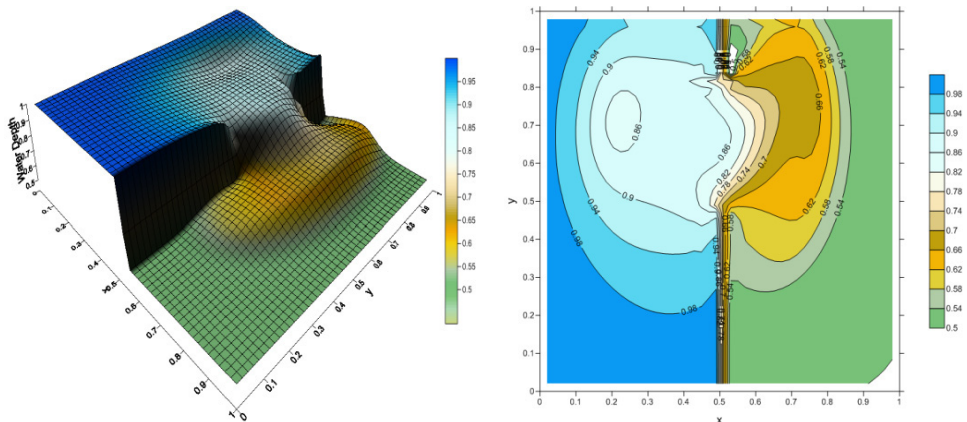


Fig. 9. (Color online) Water depth and depth contours, for the case (i) of the partial dam-break problem.

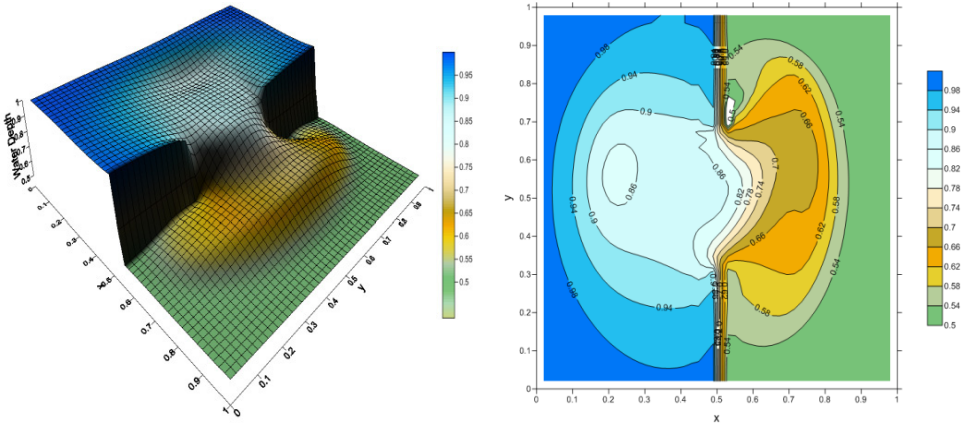


Fig. 10. (Color online) Water depth and depth contours, for the case (ii) of the partial dam-break problem.

artificial viscosity principle for solving such models even though existence of shock waves.

5. Conclusion

In this work, two numerical schemes based on method of lines and artificial viscosity concept have been developed in order to simulate one and two dimensional shallow water flows with and without source terms existing. The main feature of the proposed schemes is their robustness and simplicity. The addition of the artificial viscosity term contributed a lot in the removal of unphysical numerical oscillations and increasing the accuracy of the results. The sufficient condition for stability of the MOL I scheme is deduced as well. The considered benchmark test problems have shown that the proposed schemes offer accurate results that in good agreement with ones mentioned in literatures. The accuracy of the results demonstrate that the considered schemes are efficient, dependable, and can be of practical attention and further development when solving problems related to shallow water flows.

Acknowledgments

The first author would like to thank Deanship of Scientific Research at Majmaah University for supporting this work under Project Number No. 60/38.

References

1. A. Baghlan, *Scientia Iranica* **18**(5) (2011) 1061.
2. J. P. Boris and D. L. Book, *J. Comput. Phys.* **20** (1976) 397.
3. M. J. Castro, J. Macías and C. Parés, *ESAIM-Math. Model. Num.* **35**(1) (2001) 107.
4. P. Colella and P. Woodward, *J. Comput. Phys.* **54** (1984) 174.
5. A. J. C. De Saint-Venant, *C. R. Acad. Sci. Paris* **73** (1871) 147.

6. A. I. Delis and Th. Katsaounis, *Applied Mathematical Modelling* **29** (2005) 754.
7. L. Fraccarollo and H. Capart, *J. Fluid Mech.* **461** (2002) 1.
8. S. K. Godunov, *Mat. Sb.* **47** (1959), 271.
9. G. Hall and J. M. Watt, *Modern Numerical Methods for Ordinary Differential Equations* (Clarendon Press, Oxford, 1976).
10. A. Harten, *J. Comput. Phys.* **49** (1983) 357.
11. A. Harten, B. Enquist, S. Osher and S. R. Chakravarthy, *J. Comput. Phys.* **71** (1987) 231.
12. R. L. Higdon, *Acta Num.* **15** (2006) 385.
13. J. R. Holton, *An Introduction to Dynamic Meteorology* (Academic Press, Elsevier, Burlington, MA, 2004).
14. J. Hudson, *Numerical techniques for shallow water equations* (Numerical Analysis Report 2/99, University of Reading, 1999).
15. S. Jaisankar and S. V. Raghurama Rao, *J. Comput. Phys.* **228** (2009) 770.
16. A. Kurganov and G. Petrova, *SIAM J. Sci. Comput.* **31**(3) (2009) 1742.
17. S. Lanzoni, A. Siviglia, A. Frascati and G. Seminara, *Water Resour. Res.* **42** (2006) W06D17.
18. P. D. Lax and B. Wendroff, *Commun. Pure Appl. Math.* **13** (1960) 217.
19. D. Liang, R. A. Falconer and B. Lin, *Advances in Water Resources* **29** (2006) 1833.
20. R. W. MacCormack, *AIAA Paper* (1969) 69.
21. R. W. MacCormack, *AIAA Paper* (1981) 81.
22. M. M. Mousa and M. Reda, *Appl. Phys. Res.* **5**(3) (2013) 43.
23. M. M. Mousa, *Z. Naturforsch. A* **70** (2015) 47.
24. M. M. Mousa, *J. Ocean Eng. Sci.* **3**(4) (2018) 303.
25. P. Noble and J. P. Vila, *SIAM J. Numer. Anal.* **52**(6) (2014) 2770.
26. P. L. Roe, *J. Comput. Phys.* **43** (1981) 357.
27. W. E. Schiesser, *The Numerical Method of Lines* (Academic Press, New York, 1991).
28. W. E. Schiesser, *Comput. Math. Appl.* **28** (1994) 147.
29. J. J. Stoker, *Water Waves* (Wiley-Interscience, 1957).
30. B. Van Leer, *J. Comput. Phys.* **32** (1979) 101.
31. V. V. Ostapenko, *Doklady Physics* **63**(1) (2018) 33.
32. H. Lee, *J. Mech. Sci. Technol.* **33**(7) (2019) 3301.
33. Y. Liu, Z. Zou, L. Zou and S. Fan, *Ocean Eng.* **189** (2019) 106311.
34. C. Parés and E. Pimentel, *J. Comput. Phys.* **378** (2019) 344.
35. X. Wang, G. Li, S. Qian, J. Li and Z. Wang, *Appl. Math. Comput.* **363** (2019) 124587.